Journal of Research and Applications in Mechanical Engineering
ISSN: 2229-2152 (Print); 2697-424x (Online)
(2022) Vol. 10, No. 1, Paper No. JRAME-22-10-006
DOI: 10.14456/jrame.2022.6

Research Article

AN EXPERIMENT STUDY ON THERMAL PERFORMANCE OF AN OSCILLATING HEAT PIPE APPLY FOR LITHIUM-IRON PHOSPHATE BATTERY THERMAL MANAGEMENT SYSTEM

S. Chotmanee
S. Tundee*
Department of Mechanical Engineering, Faculty of Engineering, Rajamangala University of Technology Isan, Khonkaen Campus, Khonkaen 40000, Thailand

Received 18 February 2022
Revised 31 March 2022
Accepted 5 April 2022

ABSTRACT:
This paper presents a study on thermal performance of an oscillating heat pipe applied on lithium-iron phosphate battery thermal management system. The oscillating heat pipes were closed-loop oscillating heat pipe (CLOHP) and closed-loop oscillating heat pipe with check valve (CLOHP/CV). There are two types of working fluids in the heat pipes; R134a and R134a+TiO_2. Two types of heat sources are used in this experiment. First, lithium-iron phosphate batteries discharging. Second, a heater simulating the batteries. The experiments showed that the installation of check valve reduced the starting temperature and time when compared with CLOHP. The closed-loop oscillating heat pipe with check valve with R134a reduced the simulated batteries temperature to 55.8°C. The maximum heat transfer was 98.557 W. In case of CLOHP/CV with R134a+TiO_2, it was found that the heat pipes were in a dry-out state, resulting in an inability to maintain the temperature of the simulated battery below 60°C.

Keywords: *Oscillating heat pipe, Check valve, Heat transfer rate, Thermal resistance*

1. INTRODUCTION

Nowadays, electric vehicles (EVs) and hybrid electric vehicles (HEVs) are getting more attention. It is a new alternative for solving the energy crisis caused by the shortage of fossil fuel energy and environmental pollution caused by the internal combustion of high-carbon emission engines.

The main component of electric vehicles is the lithium-ion battery, which is a power source with high specific power densities. Lithium-ion batteries have a high capacity, suitable for long-distance driving and capable of providing fast acceleration [1]. However, the lithium-ion battery dissipates heat resulting in high battery temperatures during charging and discharging. The high temperature affects the battery's life [2] and the efficiency of the battery [3]. Management of battery temperature is challenging as overheating can cause damage to the electric vehicle systems, jeopardizing the safety of the vehicle due to potential burning of the batteries and explosions.

Therefore, the cooling technology of lithium-ion batteries is important in the development of electric vehicles [4]. Battery temperatures can be managed in many ways, for example using air cooling [5, 6], liquid (water/oil/refrigerant) cooling [7-9], phase-change materials (PCMs) [10-13], and heat pipes [4, 14-16].

* Corresponding author: S. Tundee
E-mail address: sura.tu@rmuti.ac.th

It was reported that the optimal operating temperatures of lithium-ion batteries lie in the range of 15-50°C and the temperature difference among the cells should not be over 5°C [17]. In hot and humid climates such as Thailand, battery cooling is necessary if the performance of electric vehicle is to be practically optimised. As safety is key to passengers, the popularity of electric vehicles is currently limited due to safety concerns from the overheating of batteries [18, 19]. The challenge of battery cooling is urgent to promote and accelerate the use of EVs globally [20].

Heat pipes are considered an attractive cooling technology because they can work without external power, and they can function even under relatively small temperature differences. Moreover, heat pipes are inexpensive and easy to maintain.

There have been studies on the efficiency of heat transfer of heat pipes and heat pipes with wicked internal wall [21]. Oscillating heat pipes (OHPs) require no additional material inside and they are easy to maintain, making them the most popular type of heat pipe in industry and electronic equipment. OHPs are efficient and can be applied in various uses [22]. OHPs function as a combination of several conventional thermosyphon heat pipes by the oscillatory movement of the working fluid. Heat transfer can be adjusted by increasing or decreasing the number of turns.

The oscillating heat pipe is a highly efficient heat transfer device used to test the cooling system of electric vehicle batteries [23]. To identify gaps, we conducted a literature survey on uses of heat pipes for cooling of batteries on electric vehicles. There have been some research investigations conducted on the use of OHPs for electric vehicle batteries. Rao et al. [12] designed and tested the cooling of lithium-ion batteries using an OHP using water at the condenser section and found that the temperature of the simulated battery can be kept below 50°C with a heating power supply of 50 W. In addition, Ri-Guang et al. [14] conducted a feasibility study of closed-ended OHPs. The authors examined the cooling of li-ion batteries with an OHP with 15 turns and ethanol was used as a working fluid. It was found that the temperature of the simulated battery was maintained below at 60°C. Wang et al. [21] investigated the use of an L-shaped heat pipe for managing a battery cell's temperature at both low-temperature and high temperature conditions. The condenser was mounted on an aluminium plate between the two battery cells. It was found that the performance of the L-shaped heat pipe was inferior to conventional thermosyphon heat pipes. Wei et al. [23] studied an OHP pipe for the cooling of the electric vehicle batteries by installing a copper plate at the evaporation section. Water, ethanol, and ethanol-water mixtures were studied. It was reported that the simulated battery temperature was able to stay at 46.5°C under a power input of 56 W.

Previous works present an investigation of the mixing of nanomaterials with water and other working fluids but there has been no research on the mixing nanomaterials with R1341a for an OHP. R134a has a low boiling point, making it attractive. By mixing with nanomaterials, the working fluid may increase the heat transfer further, enhancing the cooling of electric vehicle batteries.

The current research aimed to investigate the performance in the cooling of lithium-iron phosphate batteries using oscillating heat pipes with and without check valves and the use of R134a, and R134a and titanium dioxide nanoparticles as working fluids. The paper presents the experiments we conducted, the analysis and finally our conclusions.

2. EXPERIMENTAL SETUP

An oscillating heat pipe used in the process was made of copper with an internal diameter of 2.03 mm, the length of the condenser, adiabatic, and evaporator sections were equally 70 mm. The oscillating heat pipe had 3 U-turns and the curvature radii of U-turns at the evaporator and condenser are equally 12.5 mm. Two types oscillating heat pipe were studied: closed-loop oscillating heat pipe (CLOHP) and closed-loop oscillating heat pipe with check valve (CLOHP/CV). Two types of working fluids were tested: pure R134a and R134a-titanium dioxide nanoparticle mixture of 1% by volume, dubbed R134a+TiO_2. The filling ratio for both working fluids were 50%. However, there is limitation to the mixing of nanoparticles with working fluid in the OHP. The nanoparticles have a tendency to stick to the channel which will cause a pressure drop across the OHP. Even though, it was not possible to measure the corresponding pressure drop in the current work, the concentration of the nanoparticles was kept low at 10g per 1000g of R134a.

Two types of heat sources were used in this experiment; first, lithium-iron phosphate batteries discharging at a constant voltage of 6.6 V with an automatic charger with discharging ability; second, a heater simulating the batteries with adjustable input power of 20 W – 120 W. To monitor the temperature variations on the OHP as well as on the simulated EV battery, thirteen K-type thermocouples with a same diameter of 0.1 mm (±0.4 °C in accuracy) were used., as shown in Fig. 1, to analyze the heat transfer rate and thermal resistance of heat pipe. Data is sampled at a period of 1 second using a temperature recorder Yokogawa, MV1000 ±0.05°C with 24 channels and transferred to a computer. The electric heating unit provides the power input to the OHP, mainly consisting of an AC voltage stabilizer (JONCHN SVC-II), a voltage regulator (CARSPA TDGC2-1,1kVA), a power meter (FLUKE 324) and the above mentioned electric heaters. The condenser region was cooled by codling bath (EYELA CA-1115-CE).

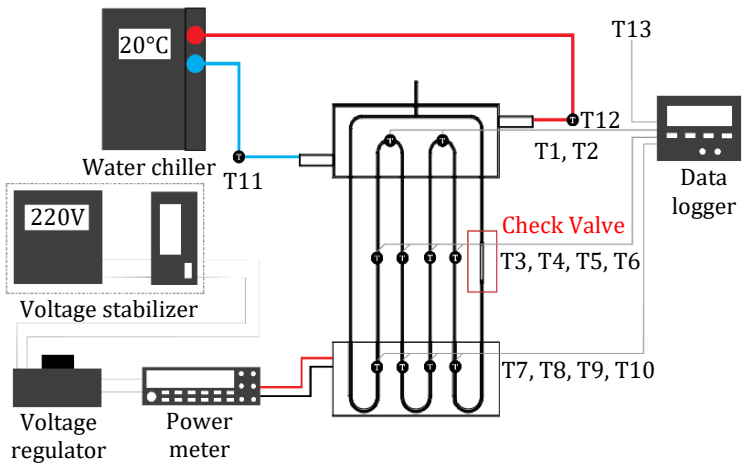

(a) Heater kit

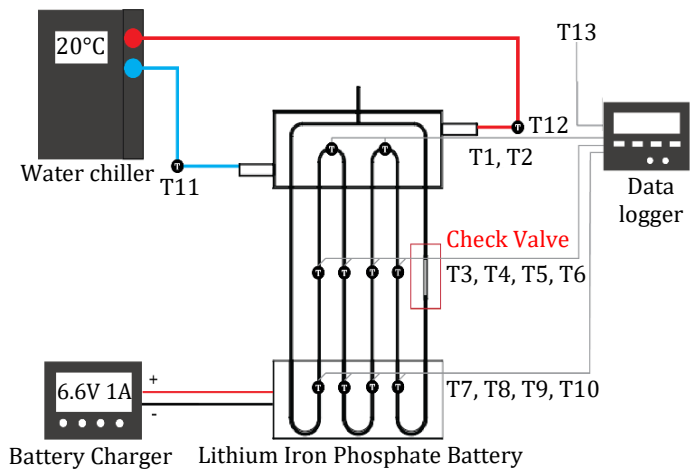

(b) $LiFePO_4$ kit

Fig. 1. Schematic diagram of the experimental setup.

As illustrated in Fig. 1, the main setup consists of 4 parts: the heating unit, cooling unit, oscillating heat pipe unit, and measurement unit. The temperatures recorded were as follows: T1 and T2 at the condenser section; T3, T4, T5 and T6 at the adiabatic section; and T7, T8, T9 and T10 at the evaporator section. T11, T12 and T13 were the inlet water to condenser, outlet water from condenser and ambient temperature, respectively.

Figure 2 shows the installation of a copper plate evaporator with 6 parallel grooves inside and a water-cooling section at the condenser section of the heat pipe. Figure 3 shows the installation of a heater plate at the evaporator section of 150x70 mm.

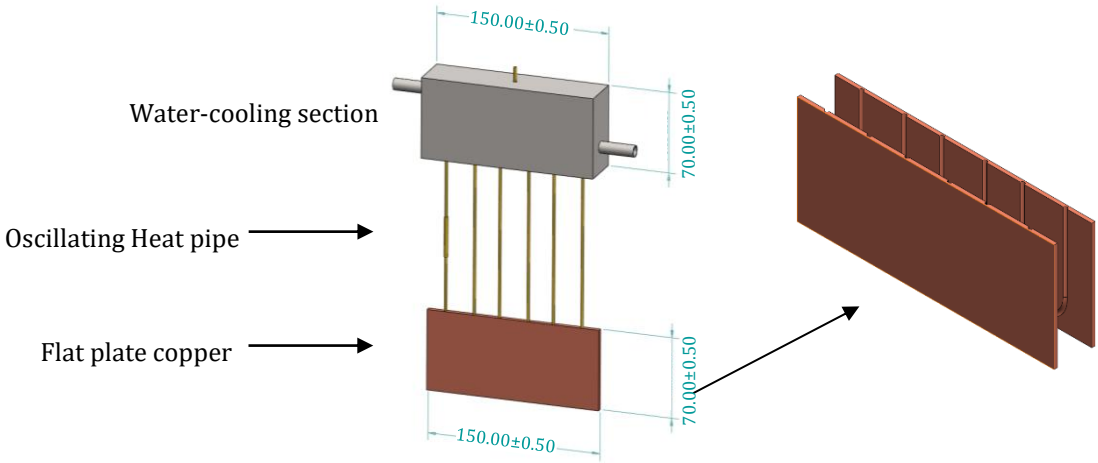

Fig. 2. Schematic diagram of OHP and flat plate copper evaporator.

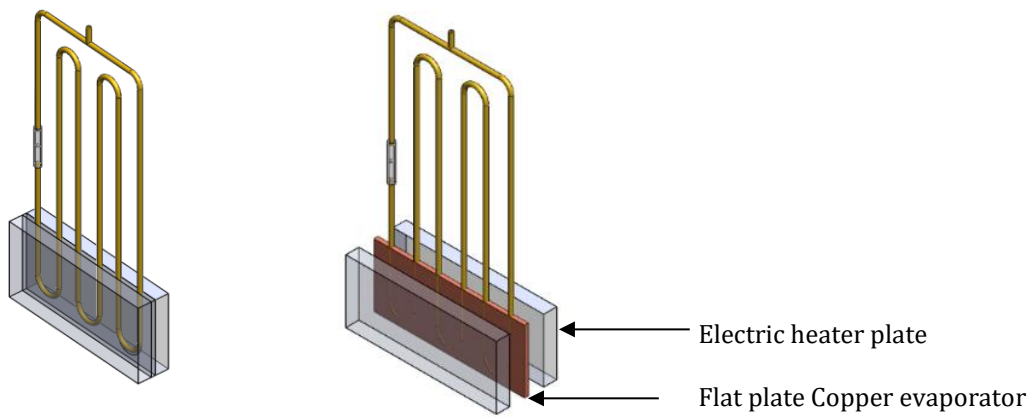

Fig. 3. Sandwich structure of copper plate evaporator and electric heater plate

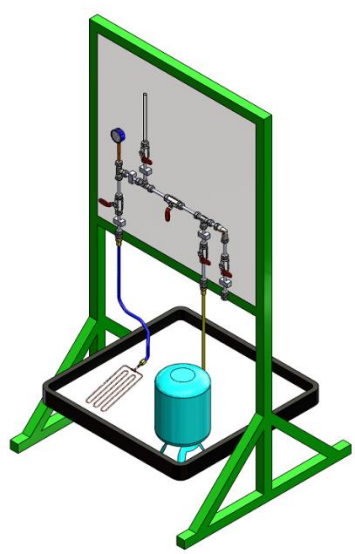

Fig 4. Schematic diagram of the OHP filling process

The filling of the working fluid was carried out according to the following steps. First, the oscillating heat pipe (OHP) was weighed prior to the filling. The OHP was then fitted to the filling machine as shown in Fig. 4. The OHP was chilled in an iced-water bath and a vacuum was created in the OHP by the vacuum pump, upon completion the machine-side valve was closed and the refrigerant-side valve was opened to allow the working fluid to fill the OHP from the tank. The OHP was then weighed again.

The increase in weight must equal the pre-calculated value from the fluid-occupying volume of 50% of the total volume of the OHP and the fluid's density. The filling ratio of 50% has previously been reported to achieve a high heat transfer by optimising the two-phase movement inside the OHP. [24, 25]

The parameters used in the experiment and the technical specification of the $LiFePO_4$ battery cell are shown in Table 1 and Table 2, respectively. Due to safety reasons, the battery was only tested at low-current discharge conditions, resulting in lower test temperatures comparable to the temperatures simulated by the heater.

Table 1: Parameters used in the experiment

Working fluid	R134a, R134a+TiO_2
Input power	20 W to 120 W
Water flow rate	0.5 LPM
Battery & Heater length	150 mm
Battery & Heater wide	70 mm
Battery thickness	25 mm
Copper plate length	150 mm
Copper plate wide	70 mm
Copper plate thickness	3 mm

Table 2: $LiFePO_4$ battery cell specification

Rate voltage	3.3 V
Rate capacity	2300mAh
Weight	710g
Minimum discharge voltage	2.5 V
Working voltage	3.0 ~ 3.2 V
Maximum charge voltage	3.65 V
Energy density	125 – 250 Wh/L
Charge Temperature	60 °C
Discharge Temperature	-20 – 60 °C
Cycle life	2,700 – 100,000 Cycle
Size	2.5×15×7 cm

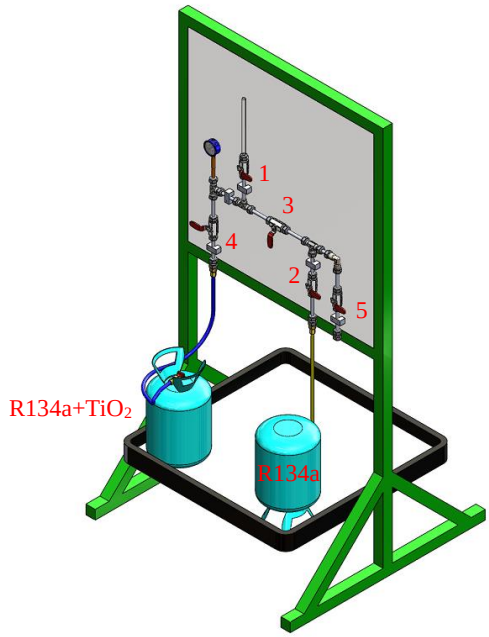

Fig. 5. Schematic diagram of mixing nano-fluid process

The mixing of the nanoparticles with the working fluid was carried out following the steps adapted from Pasha [26], illustrated schematically in Fig. 5. The R134a tank was placed upside down to ensure that the liquid instead of vapor was released from the tank for mixing. First, the entire valves were closed to create a close system. Valve number 1 was opened before 10g of titanium dioxide nanoparticles in a powder form was poured into the inlet. After closing valve number 1, the valve at the R134a tank was opened, valve number 2 and 3 were opened. Valve number 4 was opened before the valve at the mixing tank was opened. The properties of the nanoparticles are shown in Table 3. The accuracies of the equipment are shown in Table 4

Table 3: Properties of the titanium dioxide nanoparticle

Nanoparticles	TiO_2
Mean diameter(nm)	40
Density (kg/m^3)	4230
Thermal conductivity (W/m K)	11.7
Specific heat (J/kg K)	692
Melting Point (°C)	1843
Boiling Point (°C)	2972

Table 4: The accuracies of the equipment

Parameters	**Accuracy**	**Uncertainty**
Thermocouple type K	± 0.4	0.0149
Data logger	± 0.05	0.01
Power meter	1.5%±5 digits	0.006
Voltage regulator	±3	0.25
Codling bath	±2	0.0146

3. DATA PROCESSING AND MEASUREMENT UNCERTAINTIES

The overall thermal resistance which is an important parameter indicating the heat transfer performance of an OHP can be determined by Eq. (1).

$$R = \frac{T_e - T_c}{Q} \tag{1}$$

where T_c and T_e are the averaged wall temperatures of the condenser section and evaporator section, respectively, determined by Eq. (2) and Eq. (3).

$$T_c = \frac{1}{2}\sum_{i=1}^{2} Ti \tag{2}$$

$$T_e = \frac{1}{4}\sum_{i=7}^{10} Ti \tag{3}$$

where Ti (i=1, 2, 3, ..., 10) are wall temperatures measured by the thermocouples allocated at different regions of the OHP as illustrated in Fig. 1 and Q is the heating power added to the evaporator section determined by Eq. (4)

$$Q = UI \tag{4}$$

where U and I are the input voltage and electric current, respectively.

To deal with measurement uncertainties inherent in Eq. (1) and (4), the error propagation principle has been applied. The uncertainties in the parameter R and Q can be expressed in Eq. (5) and Eq. (6), respectively.

$$\frac{\Delta Q}{Q} = \sqrt{\left(\frac{\Delta I}{I}\right)^2 + \left(\frac{\Delta U}{U}\right)^2} \tag{5}$$

$$\frac{\Delta R}{R} = \sqrt{\left(\frac{(\Delta T_e)^2 + (\Delta T_c)^2}{(T_e - T_c)^2}\right) + \left(\frac{\Delta Q}{Q}\right)^2} \tag{6}$$

The heat transfer rate at the condenser section is calculated using Eq. (7).

$$Q_c = \dot{m} C_p \left(T_{out} - T_{in}\right) \tag{7}$$

where $\dot{m}$ and C_p are the mass flow rate and specific heat of the fluid, respectively.

4. RESULTS AND DISCUSSION

4.1 Operating characteristics of OHP

As a reference, the heat transfer performance of empty OHP (namely 0% filling ratio) was also tested. From Fig. 3, the heat source was adjusted every 10 minutes to heat power of 20 W, 40 W, 60 W, 80 W, 100 W, and 120 W. From Fig. 6, it can be seen that the evaporator temperatures increased with the power input and eventually were close to 158.6°C at 120 W. The reason for the adjusted input power of 120 W was due to the thermal runaway of the battery was observed at high temperatures while the condenser temperatures were slightly increased. Theoretically, the imposed input power was largely transported by means of heat conduction through the wall of the copper tube due to the absence of refrigerant and dissipated at the condenser region through convection and radiation.

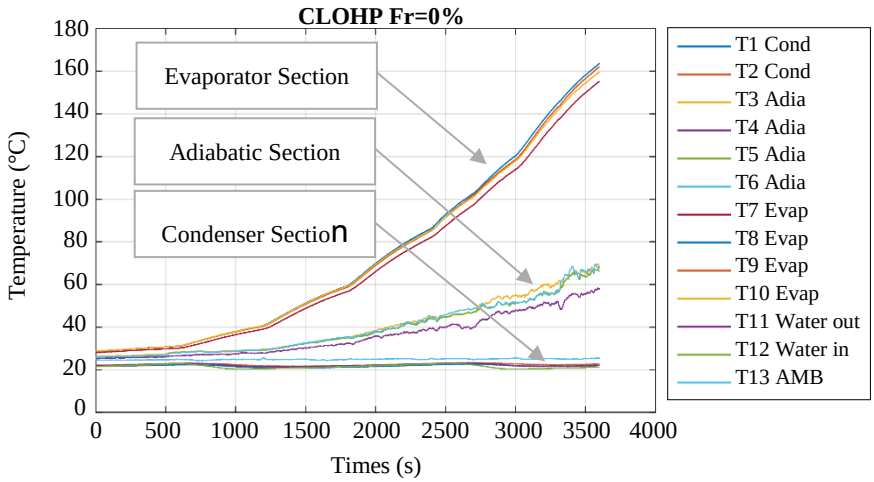

Fig. 6. Temporal temperature variations of empty OHP vs. times (FR=0%)

4.2 Experiment with heater

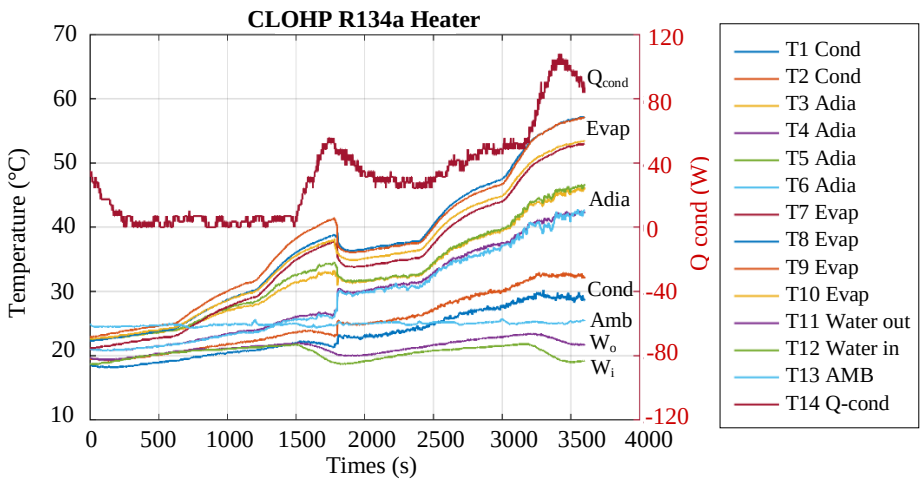

(a) CLOHP

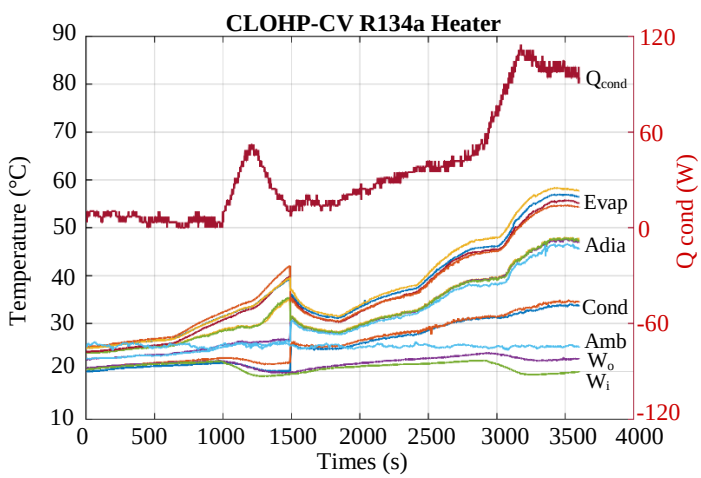

(b) CLOHP/CV

Fig. 7. Temporal temperature variations of OHP vs. times [R134a] (a) CLOHP; (b) CLOHP/CV

Figure 7 (a) and (b) shows the temperature of the oscillating heat pipe with R134a as compared with time. It shows that the evaporating average temperature and startup time of the closed-loop oscillating heat pipe with check valve (CLOHP/CV) were lower than the closed-loop oscillating heat pipe (CLOHP) without check valve. The installed check valve forced the working fluid to flow in the same direction throughout.

The CLOHP/CV showed an average startup working temperature of 39.3°C whereas the startup time was 24.49 minutes, the CLOHP's average startup temperature was 40.2°C and the startup time was 29.52 minutes. It was found that both heat pipes started in the 60 W heating range, which was initiated during the moderate heat supply medium and high.

The analysed ratio of heat transfer of the heat pipes was the heat supply range of 120 W at the highest temperature range. The CLOHP/CV's heat transfer was measured to be 98.55 W, maintaining the average temperature at the evaporator section at 55.8 °C. In contrast, the CLOHP's heat transfer was 77.24 W which kept the average temperature at the evaporator section at 57.2 °C.

The observations demonstrated that the oscillating heat pipes with R134a could control the temperature of the evaporator section to below 60°C, which is the temperature limit for optimal battery operation.

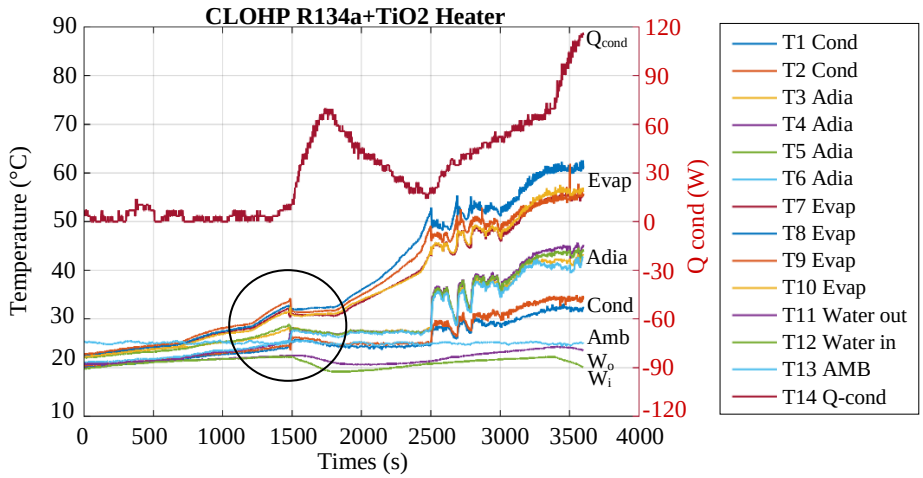

(a) CLOHP

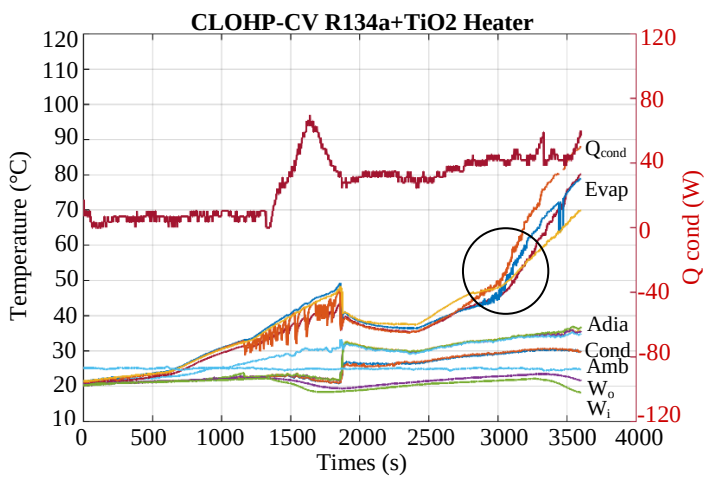

(b) CLOHP/CV

Fig. 8. Temporal temperature variations of OHP vs. times [R134a+TiO_2] (a) CLOHP; (b) CLOHP/CV

Figure 8 shows the temperature of the oscillating heat pipe with titanium dioxide nanoparticle mixtures of 1% by volume as R134a+TiO_2 has resulted in a more viscous working fluid. When titanium dioxide nanoparticle mixtures as the state of the active substance changes. As a result, the boiling point of the working fluid was increased.

The startup temperature and startup time are therefore increased, with a CLOHP/CV having an average startup temperature of 47.1°C, a startup time of 30.58 minutes, and a CLOHP with an average startup temperature at 47.1°C. and startup time 41.39 minutes. CLOHP/CV can be seen starting in the 80 W range, while a CLOHP was starting at 100 W. Obviously, the installation of check valve affects the temperature and startup time of the heating pipes.

Figure 8 (a) shows a slight change in temperature similar to the startup of a heat pipe. There was a brief vibration of the working fluid at the evaporator section an average temperature at 33.7°C. The temperature continued to rising than the point where the heat pipe started operating at an average at 48.4°C due to the instability of the working fluid. At the 120 W power supply CLOHP, the temperature can be maintained at 57.2°C.

From Fig. 8 (b), during the 100 W power supply, the mean temperature of the evaporator section increased abnormally. However, the average temperature of the condenser section was unchanged. Thus, it explains that the CLOHP/CV experienced a dry out state as a result of the increase in temperature at the evaporation section causing the active substance vapor to expand as it moved to the condenser section, it flows counter to the liquid and vapor moving from the condenser section down to the evaporator section, causing the resistance of the working fluid to move. Including titanium dioxide nanoparticles that are insoluble in water causes the check valve to become clogged due to agglomeration. When working fluid is unable to flow in the direction forced with check valve. CLOHP/CV results in the working fluid at the evaporator section drying up, resulting in a 120 W power supply. The temperature rises to 84.1°C.

4.3 Experiment with lithium iron phosphate batteries

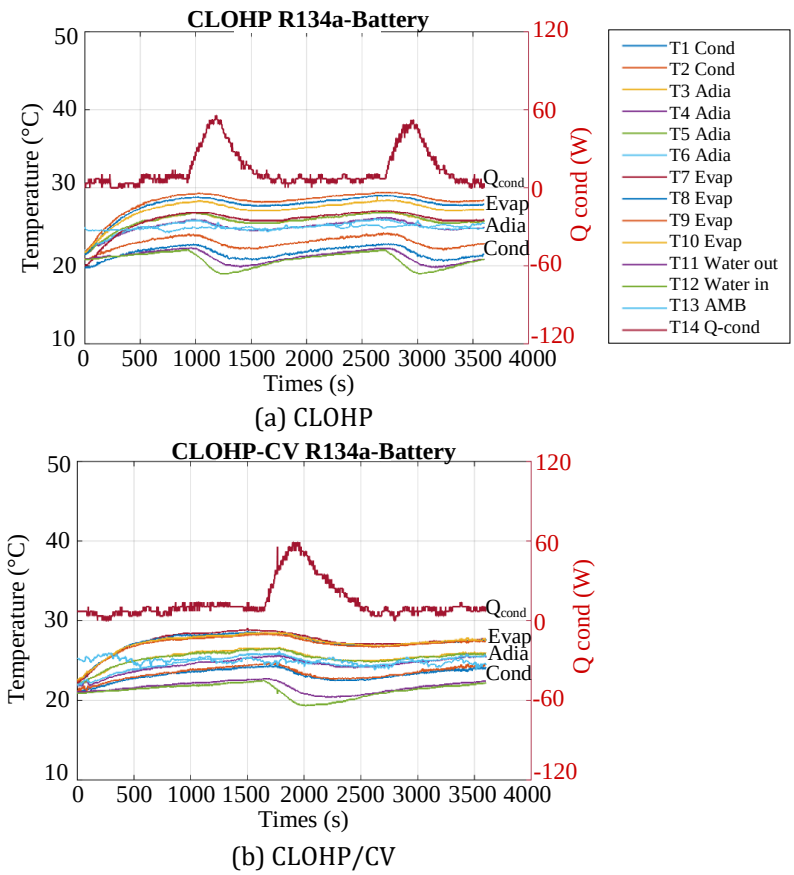

Fig. 9. Temporal temperature variations of OHP vs. times [R134a] (a) CLOHP; (b) CLOHP/CV

Figure 9 shows the temperature of the oscillating heat pipe with R134a versus time using heat source by lithium-iron phosphate batteries with constant discharge rate at current discharge 1 A and voltage discharge 6.6 V, which is a test by discharging at low current, so there was less change in temperature and found that the temperature of the heat pipe in the evaporator section was not high that making it impossible to determine the startup of the heat pipe as compared to the case of using a heater. However, it can be seen that the average temperature at startup at 30°C - 40°C and the heat source was increased, the heat pipe was also able to cooling a lithium-iron phosphate batteries and can keep the temperature in the range suitable for discharging the batteries.

The lithium-iron phosphate batteries had heat transfer values of CLOHP/CV and CLOHP with R134a of 14.13 W and 13.92 W, respectively. The battery temperature can be maintained at 28.7°C and 29.4°C, respectively. Which, the optimum temperature range for lithium-iron phosphate batteries operation.

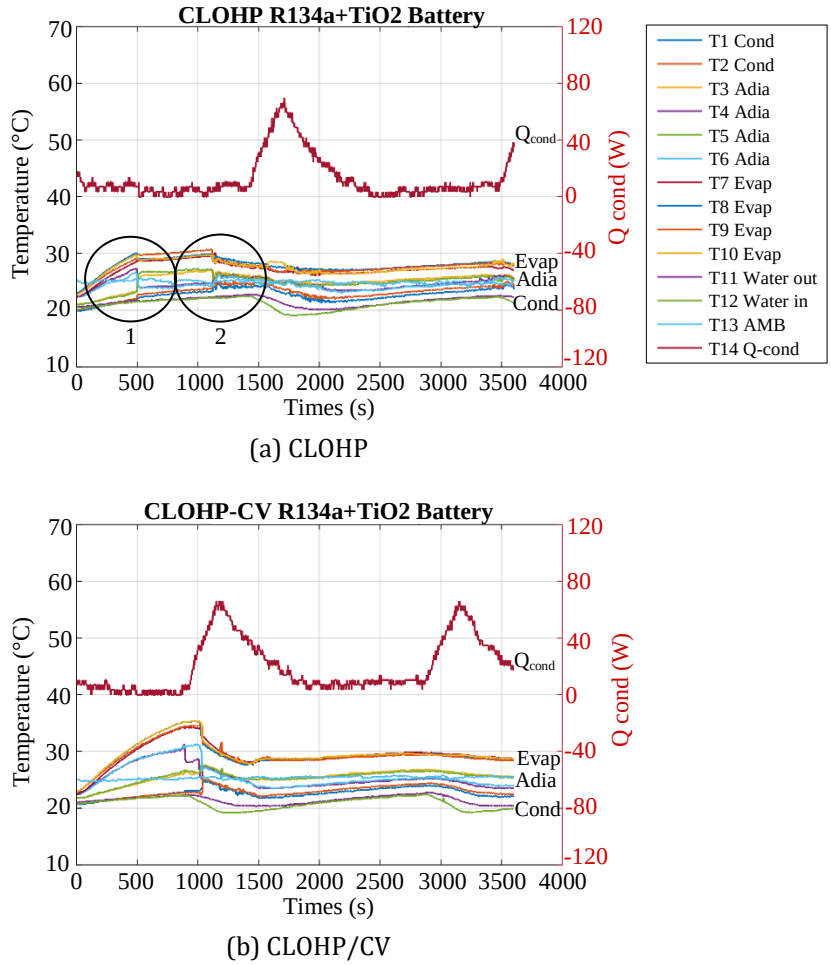

Fig. 10. Temporal temperature variations of OHP vs. times [R134a+TiO_2] (a) CLOHP; (b) CLOHP/CV

Figure 10 shows the temperature of the oscillating heat pipe with R134a+TiO_2 versus time using heat source by lithium-iron phosphate batteries with constant discharge rate at current discharge 1 A and voltage discharge 6.6 V, was found that when changing the working fluid from R134a to R134a+TiO_2 the average temperature of the heat pipe surface at the evaporator section was higher. As the temperature increases, the working fluid inside was boils and the cumulative vapor pressure of the working fluid becomes enough to startup. Then, when the oscillating heat pipe in operation, the temperature of the evaporator section decreases. Conversely, the heat pipe surface temperature at the condenser section increases and approaches a steady state.

The addition of the working fluid R134a+TiO_2 filled with TiO_2 nanoparticles at a rate of 1.0% by volume increased the viscosity of the working fluid, resulting from an increase in the boiling point of the working fluid. Thus, the temperature of the evaporator section rises until the working fluid boils, resulting in the heat transfer to the lower temperature condenser section.

The oscillating heat pipe was startup as the heat transfer values of CLOHP/CV and CLOHP were 19.375 W and 12.650 W, respectively. And the startup time of 17.11 minutes and 18.33 minutes, respectively. The CLOHP/CV has a lower startup time than CLOHP, as in the case of heater had a result of the flow into the same direction of the working fluid inside not create resistance against the flow of the working fluid inside the pipe from Fig. 10 (b). In the case of CLOHP found the temperature changes as 2 points were observed similar to the oscillate of the working fluid inside the heat pipe. The heat pipe was started, in which the first change the temperature of the evaporator section does not decrease, which is just the unstable oscillation of the working fluid that occurs inside the heat pipe. It was found that the heat pipe was started in point 2, and it was found that the CLOHP was able to maintain the maximum temperature of the lithium-iron phosphate batteries at 29.9°C. This is better than the CLOHP/CV at 34.5°C. However, the maximum temperature of both heat pipes was within the proper operating range of the lithium-iron phosphate batteries.

4.4 Thermal resistance of OHP

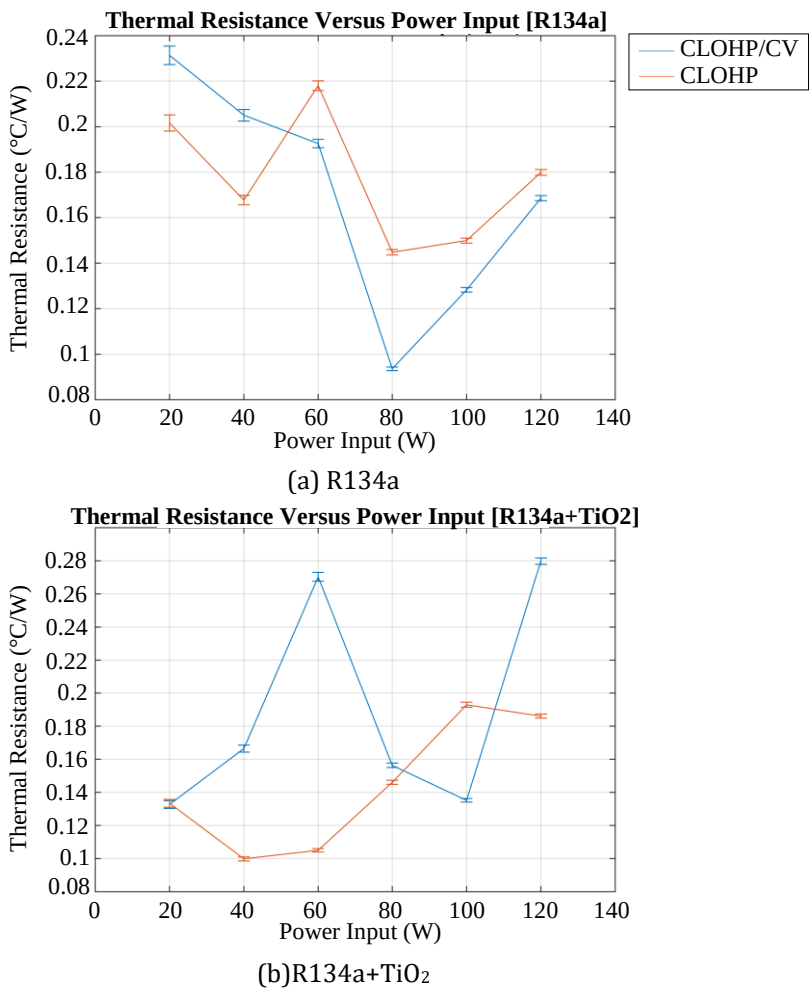

(a) R134a

(b)R134a+TiO_2

Fig. 11. Thermal resistance vs. power input of OHP filled with different working fluid (a) R134a; (b)R134a+TiO_2

Figure 11 (a) shows the changing in thermal resistance of heat pipes from heat sources when using OHP with the addition of R134a. It was found that during the power supply of 20 W to 40 W, the thermal resistance was decreased. When heated at 60 W was found that the thermal resistance of the closed-loop oscillating heat pipe was increased due to the larger difference in temperature at the evaporator section and condenser section.

As a result of adding more power supply to the heater, the heat pipes have not started. The causing temperature of the evaporator to rise after increasing the heating power at 80 W, it was found that the thermal resistance of the oscillating heat pipes was decreased due to the startup of the heat pipes and when increasing the heat supply at 100 W- 120 W, the difference in the tube surface temperature at the evaporator section and condenser section was greater. Finally, the thermal resistance was also increased.

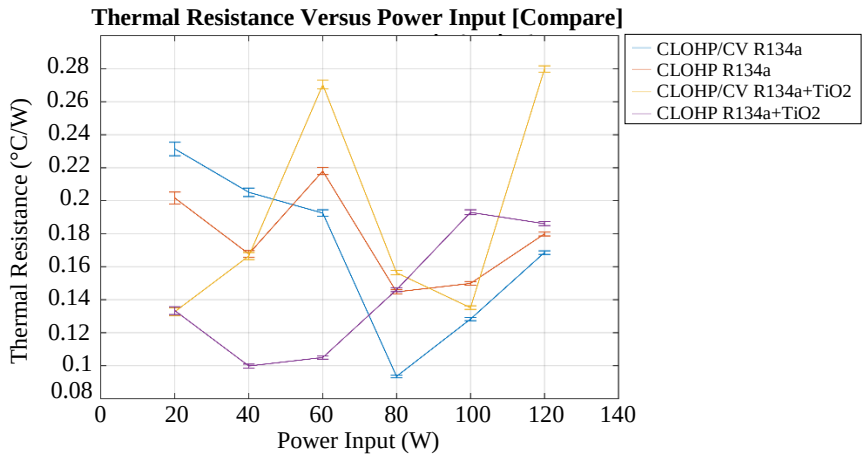

Fig. 12. Thermal resistance of OHP vs. power input at different type of OHP and working fluid

From Fig.11 (b) shows the heat source supply at 20 W to 40 W the thermal resistance decreases due to the initial unstable vibration of the working fluid as in Fig. 8 (b). When increased the heat source of 60 W the thermal resistance was increasing until 100 W It found the thermal resistance value to decrease as the heat pipe startup. Thus, the difference in temperature of the evaporator section and condenser section was reduced when compared with a CLOHP/CV. The thermal resistance of the heat pipe was increasing cause the heat pipe has not started. Until the heating power supply was increased to 80 W, it can be seen that when the heat pipe was started, the thermal resistance value will be lower when the heat source was added to 100 W, the thermal resistance was greatly increased due to the CLOHP/CV was dry out state, causing the working fluid inside the heat pipe at the evaporator section to dry, resulting in a higher evaporator section temperature. The evaporator section was higher because heat cannot be transferred to the condenser section. The difference in temperature of the evaporator and condenser sections increases, thereby increasing the thermal resistance of the tubes.

Figure 12 shows a comparison between the thermal resistances of the oscillating heat pipes with R134a and R134a+TiO_2 functional with a timing of a CLOHP/CV filled R134a+TiO_2 that added to the pipe as the highest thermal resistance of 0.270°C/W. Due to, filled with TiO_2 nanoparticle at 1.0% by volume that made the working fluid more viscous and slower boiling when compared to working fluid filled with R134a.

Therefore, the heat pipe takes longer to startup after the heat pipes were started. It was found that when the heat source at 120 W and the pipes experienced a dry-out state causing the thermal resistance to be the highest at 0.279°C/W. The lowest thermal resistance was a CLOHP/CV with R134a when the pipes are the same working fluid. The startup had the lowest thermal resistance of 0.093°C/W at the highest experimental heat source at 120 W. This type of heat pipe also has the lowest thermal resistance.

It was found that when the heat pipes have a low thermal resistance, the heat transfer from the evaporator section to the condenser section was the best, indicating the heat transfer efficiency of that heat pipe by a CLOHP/CV filled R134a was the best heat transfer rate.

5. CONCLUSION

In the case of a heater simulating the batteries, the effect on heat transfer rate and thermal resistance values of installing a check valve on the oscillating heat pipe was found. With R134a as a working fluid, the check valve resulted in a faster startup time than with no check valve. Moreover, the installation of check valve increased the heat transfer values at a heat supply power of 120 W, capable of maintaining the simulated battery at 55.8°C, which is below the maximum optimal operating temperature of the lithium-iron phosphate battery of 60°C. The highest heat transfer value of 98.55 W.

In contrast, the closed-loop oscillating heat pipe with a check valve with R134a+TiO_2 as a working fluid, dry-out occurred at heat supply power of 100 W. Reduced heat transfer rate and cooling capability were observed, with the simulated battery's temperature of 84.1°C, rendering it unable to achieve the optimal temperature limit.

In the case of lithium-iron phosphate batteries, the result showed that closed-loop oscillating heat pipe with a check valve exhibited a faster startup time than the closed-loop oscillating heat pipe without a check valve. When testing with R134a+TiO_2, it was found that the addition of titanium dioxide nanoparticles resulted in reduced cooling, resulting in a higher battery temperature than when using pure R134a. It was found that the maximum battery temperatures were 28.7°C and 34.5°C, for the pure R134a and the R134a+TiO_2 respectively. Due to safety reasons, the battery was only tested at low-current discharge conditions, resulting in lower test temperatures as compared to the simulated battery case. The maximum temperature of the simulated battery of 158.6°C at 120 W power was successfully cooled to below the required 60°C by the installation of the oscillating heat pipe. Therefore, our work shows that oscillating heat pipes may be a potential technique for the cooling and thermal management of lithium-iron phosphate batteries to allow the batteries to operate within the appropriate range for electric vehicles.

For future work, we recommend investigating the impact of nanoparticle concentration on the pressure drop across the OHP and the resulting heat transfer performance. Moreover, the battery discharging regimes may be an important factor in the thermal behaviour of the batteries. Tests should be performed to understand the cooling performance of the OHP of the battery under different discharge conditions such as constant voltage, constant current, and high discharge currents.

NOMENCLATURE

Q	heat transfer rate, W
C_p	specific heat of fluid, J/kg-K
$\dot{m}$	mass flow rate, kg/s
R	thermal resistance, °C/W
T	temperature, °C
T_e	temperature of evaporator section, °C
T_c	temperature of condenser section, °C
OHP	oscillating heat pipe
CLOHP	closed-loop oscillating heat pipe
CLOHP/CV	closed-loop oscillating heat pipe with check valve
CV	check valve
PCM	phase change material

Subscripts

evap	evaporator section
cond	condenser section
adia	adiabatic section
amb	ambient
i	inlet
o	outlet

REFERENCES

[1] Burban, G., Ayel, V., Alexandre, A., Lagonotte, P., Bertin, Y. and Romestant, C. Experimental investigation of a pulsating heat pipe for hybrid vehicle applications, Applied Thermal Engineering, Vol. 50, 2013, pp. 94-103.

[2] Duan, X. and Naterer, G.F. Heat transfer in phase change materials for thermal management of electric vehicle battery modules, International Journal of Heat and Mass Transfer, Vol. 53, 2010, pp. 5176-5182.

[3] Li, W., Chen, S., Peng, X., Xiao, M., Gao, L., Garg, A., et al. A Comprehensive approach for the clustering of similar-performance cells for the design of a lithium-ion battery module for electric vehicles, Engineering, Vol. 5, 2019, pp. 795-802.

[4] Huang, Q., Li, X., Zhang, G., Zhang, J., He, F. and Li, Y. Experimental investigation of the thermal performance of heat pipe assisted phase change material for battery thermal management system, Applied Thermal Engineering, Vol. 141, 2018, pp. 1092-1100.

[5] Jin, L.W., Lee, P.S., Kong, X.X., Fan, Y. and Chou, S.K. Ultra-thin minichannel LCP for EV battery thermal management, Applied Energy, Vol. 113, 2014, pp. 1786-1794.

[6] Xiaoming, X., Wei, T., Jiaqi, F., Donghai, H. and Xudong, S. The forced air-cooling heat dissipation performance of different battery pack bottom duct, International Journal of Energy Research, Vol. 42(12), 2018, pp. 3823-3836.

[7] Li, K., Yan, J., Chen, H. and Wang, Q. Water cooling based strategy for lithium-ion battery pack dynamic cycling for thermal management system, Applied Thermal Engineering, Vol. 132, 2019, pp. 575-585.

[8] Panchal, S., Khasow, R., Dincer, I., Agelin-Chaab, M., Fraser, R. and Fowler, M. Thermal design and simulation of mini-channel cold plate for water cooled large sized prismatic lithium-ion battery, Applied Thermal Engineering, Vol. 122, 2017, pp. 80-90.

[9] Qu, J. and Wang, Q. Experimental study on the thermal performance of vertical closed-loop oscillating heat pipes and correlation modelling, Applied Energy, Vol. 112, 2013, pp. 1154-1160.

[10] Qu, J., Wang, C., Li, X. and Wang, H. Heat transfer performance of flexible oscillating heat pipes for electric/ hybrid electric vehicle battery thermal management, Applied Thermal Engineering, Vol. 135, 2018, pp. 1-9.

[11] Rao, Z., Wang, S. and Zhang G. Simulation and experiment of thermal energy management with phase change material for ageing LiFePO4 power battery, Energy Conversion and Management, Vol. 52, 2011, pp. 3408-3414.

[12] Rao, Z., Huo, Y. and Liu, X. Experimental study of an OHP-cooled thermal management system for electric vehicle power battery, Experimental Thermal and Fluid Science, Vol. 57, 2014, pp. 20-26.

[13] Zhao, J., Rao, Z., Liu, C. and Li, Y. Experimental investigation on thermal performance of phase change material coupled with closed-loop oscillating heat pipe (PCM/CLOHP) used in thermal management, Applied Thermal Engineering, Vol. 93, 2016, pp. 90-100.

[14] Ri-Guang, C., Won-Sik, C. and Seok-Ho, R. Thermal characteristics of an oscillating heat pipe cooling system for electric vehicle li-ion batteries, Energies, Vol. 11(3), 2018, pp. 1-16.

[15] Sabbah, R., Kizilel, R., Selman, J.R. and Al-Hallaj, S. Active (air-cooled) vs. passive (phase change material) thermal management of high-power lithium-ion packs: limitation of temperature rise and uniformity of temperature distribution, Journal of Power Sources, Vol. 182, 2008, pp. 630-638.

[16] Tran, T.H., Harmand, S. and Sahut, B. Experimental investigation on heat pipe cooling for hybrid electric vehicle and electric vehicle lithium-ion battery, Journal of Power Sources, Vol. 265, 2014, pp. 262-272.

[17] Wang, Q., Jiang, B., Li, B. and Yan, Y. Critical review of thermal management models and solutions of lithium-ion batteries for the development of pure electric vehicles, Renewable and Sustainable Energy Reviews, Vol. 64, 2016, pp. 106-128.

[18] Kim, J., Oh, J. and Lee, H. Review on battery thermal management system for electric vehicles, Applied Thermal Engineering, Vol. 149, 2018, pp. 192-212.

[19] Lu, M., Zhang, X., Ji, J., Xu, X. and Zhang, Y. Research progress on power battery cooling technology for electric vehicles, Journal of Energy Storage, Vol. 27, 2022, Article number: 101155.

[20] Kulranut, J., Dapaiwa, N., Yenwichai, T., Intano, W. and Masomtob, M. Improvement of estimation method for battery cell heat generation, Journal of Research and Applications in Mechanical Engineering, Vol. 9(2), 2021, pp. 1-10.

[21] Wang, Q., Jiang, B., Xue, Q.F., Sun, H.L., Li, B., Zou, H.M., et al. Experimental investigation on EV battery cooling and heating by heat pipes, Applied Thermal Engineering, Vol. 88, 2015, pp. 54-60.

[22] Wang, Q., Rao, Z., Huo, Y. and Wang, S. Thermal performance of phase change material/oscillating heat pipe-based battery thermal management system, International Journal of Thermal Sciences, Vol. 102, 2016, pp. 9-16.
[23] Wei, A., Qu, J., Qiu, H., Wang, C. and Cao, G. Heat transfer characteristics of plug-in oscillating heat pipe with binary-fluid mixtures for electric vehicle battery thermal management, International Journal of Heat and Mass Transfer, Vol. 135, 2019, pp. 746-760.
[24] Qu, J., Wu, H., Cheng, P. and Wang, X. Non-linear analyses of temperature oscillations in a closed-loop pulsating heat pipe, International Journal of Heat and Mass Transfer, Vol. 52, 2009, pp. 3481-3489.
[25] Guo, C., Wang, T., Guo, Ch., Jiang, Y., Tan, S. and Li, Z. Effects of filling ratio, geometry parameters and coolant temperature on the heat transfer performance of a wraparound heat pipe, Applied Thermal Engineering, Vol. 200, 2022, Article number: 117724.
[26] Pasha, MK. Controlling the Nusselt number in a TiO2/R134a nano-refrigerant System, International Journal of Heat and Technology, Vol. 37(1), 2019, pp. 179-187.